analytical chemistry

THE UNIVERSITY OF MEMPHIS. University Libraries

Subscriber access provided by University Libraries, University of Memphis

Article

Characterization of a New Anticancer Agent, EAPB0203 and its Main Metabolites: Nuclear Magnetic Resonance and Liquid Chromatography-Mass Spectrometry studies

Florian Lafaille, Bernard Banaigs, Nicolas Inguimbert, Christine Enjalbal, Pierre-Emmanuel Doulain, Pierre-Antoine Bonnet, carine Deleuze-Masquefa, and Francoise MM BRESSOLLE

Anal. Chem., **Just Accepted Manuscript** • Publication Date (Web): 17 Oct 2012

Downloaded from http://pubs.acs.org on October 23, 2012

Just Accepted

"Just Accepted" manuscripts have been peer-reviewed and accepted for publication. They are posted online prior to technical editing, formatting for publication and author proofing. The American Chemical Society provides "Just Accepted" as a free service to the research community to expedite the dissemination of scientific material as soon as possible after acceptance. "Just Accepted" manuscripts appear in full in PDF format accompanied by an HTML abstract. "Just Accepted" manuscripts have been fully peer reviewed, but should not be considered the official version of record. They are accessible to all readers and citable by the Digital Object Identifier (DOI®). "Just Accepted" is an optional service offered to authors. Therefore, the "Just Accepted" Web site may not include all articles that will be published in the journal. After a manuscript is technically edited and formatted, it will be removed from the "Just Accepted" Web site and published as an ASAP article. Note that technical editing may introduce minor changes to the manuscript text and/or graphics which could affect content, and all legal disclaimers and ethical guidelines that apply to the journal pertain. ACS cannot be held responsible for errors or consequences arising from the use of information contained in these "Just Accepted" manuscripts.

ACS Publications
High quality. High impact.

Analytical Chemistry is published by the American Chemical Society. 1155 Sixteenth Street N.W., Washington, DC 20036

Published by American Chemical Society. Copyright © American Chemical Society. However, no copyright claim is made to original U.S. Government works, or works produced by employees of any Commonwealth realm Crown government in the course of their duties.

Characterization of a New Anticancer Agent, EAPB0203 and its Main Metabolites: Nuclear Magnetic Resonance and Liquid Chromatography-Mass Spectrometry studies

Florian Lafaille[1], Bernard Banaigs[3], Nicolas Inguimbert[3†], Christine Enjalbal[4†], Pierre-Emmanuel Doulain[2], Pierre-Antoine Bonnet[2], Carine Masquefa[2*], Françoise M.M. Bressolle[1*]

[1]Clinical Pharmacokinetic Laboratory and [2]Pharmacochemistry and Biomolecule Laboratory, EA4215, Montpellier I University, Faculty of Pharmacy, 15 Avenue Ch. Flahault, 34093 Montpellier Cedex 5, France; [3]Biochemistry and Environment Laboratory, EA 4215, Perpignan University, 52 Avenue P. Alduy, 66860 Perpignan Cedex 9, France; [4]Institut des Biomolécules Max Mousseron (IBMM), UMR 5247, Universités Montpellier 1 et 2, CNRS, Bâtiment Chimie (17), Université Montpellier 2, Place Eugène Bataillon, 34095 Montpellier Cedex 5, France

†N I and C E contributed equally to this work.

* Corresponding author E-mail:

fbressolle@yahoo.fr (**tel**.) (33) 4 11 75 95 76; (**fax)** (33) 4 11 75 97 37.

carine.masquefa@univ-montp1.fr **(tel)** (33) 4 11 75 95 36; **(fax)** 33 4 11 75 95 53

Abstract: 194 words; text: 4949 words; number of references: 13; number of tables: 1; number of figures: 2

Supplemental data: 9 figures; 2 tables; 1 text.

Abstract

The present study was conducted to assess the structures of the main unknown oxygenated metabolites of **EAPB0203**. The first step was to assign all the ^{1}H and ^{13}C nuclear magnetic resonances (NMR) of both **EAPB0203** and its demethylated metabolite (**EAPB0202**) to the corresponding atoms in their molecular structures and to elucidate the fragmentation pathways for the $[M+H]^+$ ions of these compounds using high-resolution mass spectrometry (MS). MS-MS spectra showed that both protonated molecules possessing an even number of electrons were unexpectedly losing radicals such as $H^{\bullet}$, $CH_3^{\bullet}$ or even $C_7H_7^{\bullet}$ giving stable radical cations. In vitro metabolism studies were investigated in rat and dog liver microsomes and in the filamentous fungus *Cunninghamella elegans*. Structural elucidation of six oxygenated metabolites was performed based on (i) their fragmentation pathways in liquid chromatography-MS/MS analyses; (ii) comparison of their changes in their molecular masses and fragment ions with those of the parent drugs; and (iii) the results of on-line H/D exchange experiments which provided additional evidence in differentiating hydoxylated metabolites from N-oxides. Structures of the metabolites were elucidated by LC-MS/MS and comparison with synthetic standards; structures of these standards were confirmed using 1- and 2-D1 H NMR spectroscopy.

A new series of compounds has been synthesized by our group. These compounds are analogs of imiquimod, the first member of the imidazoquinoline family, efficacious as a topical therapy for certain types of skin cancers.[1,2] The cytotoxic activity of these new compounds has been evaluated, in vitro, against human cancer cell lines. Among them, **EAPB0203** and **EAPB0503,** belonging to the imidazo[1,2-*a*]quinoxaline series, have emerged as the most promising drugs with interesting antitumoral activities against melanoma, T-lymphoma, colon and breast cancer cell lines.[3-8] In a mice melanoma model, **EAPB0203** was more potent than fotemustine.[3,7] Some data are now available on the pharmacokinetics of these compounds.[7,8]

The present paper deals with the metabolism of **EAPB0203**. In vitro metabolism studies carried out using hepatic microsomes from four mammalian species have previously shown that **EAPB0203** was metabolized via two main metabolic pathways (supplemental Figures 1 and 2): first, *N*-demethylation leading to the formation of **EAPB0202** exhibiting similar in vitro cytotoxicity against A375 melanoma cancer cell line as the parent compound;[3] second, arousing through a series of hydroxylation and/or *N*-oxidation leading to the formation of three major compounds named M2, M6 and M7 and their corresponding demethylated products, M1, M3 and M5.[8] A minor metabolite (M4) was only detected in mouse. The percentage of each metabolite according to the species is provided in supplemental data Figure 2. Unfortunately, in this previous paper,[8] the precise position of the oxygen atom has not been elucidated. Thus, the objective of the present paper was to characterize the major oxygenated metabolites of **EAPB0203**.

In the present study, several spectroscopic approaches such as nuclear magnetic resonance (NMR) and liquid chromatography-tandem mass spectrometry (LC-MS/MS) with

triple quadrupole (QqQ) and QqTof mass analyzer configurations allowing on-line mass measurement of precursor and product ions, were used to identify the main unknown oxygenated metabolites of **EAPB0203** (i.e., M1, M2, M3, M5, M6 and M7). To facilitate elucidation of metabolite structures, the first step of this work was to assign all the ^{1}H and ^{13}C NMR resonances of **EAPB0203** and **EAPB0202** to the corresponding atoms in their molecular structures, and to characterize fragmentation pathways and to identify product ions of both compounds in MS/MS. Moreover, hydrogen/deuterium (H/D) exchange experiments were performed in MS/MS to aid in identification of the metabolites.[9,10] To generate these metabolites, in vitro metabolism studies were first investigated in rat and dog hepatic microsomes, the two species metabolizing **EAPB0203** at higher rates.[8] Then, **EAPB0203** and **EAPB0202** were incubated with *Cunnighamella elegans,* a relevant in vitro model for drug metabolism studies allowing the formation of large amounts of metabolites.[11]

■ EXPERIMENTAL SECTION

Solvents, Chemicals and Reagents. **EAPB0203** (*N*-methyl-1-(2-phenethyl)imidazo[1,2-*a*]quinoxalin-4-amine; molecular weight, 302) and its demethylated metabolite, **EAPB0202,** (1-(2-phenethyl)imidazo[1,2-*a*]quinoxalin-4-amine; molecular weight, 288) were synthesized by the Pharmacochemistry and Biomolecule Laboratory (Montpellier I University, France).[12] Their structures are presented in supplemental Figure 1; each compound may exist in tautomeric forms. **EAPB0203** and **EAPB0202** were stored at 20 °C protected from light. Acetonitrile and methanol (Carlo Erba, Val de Reuil, France), ammonium formate (Fluka, Vandoeuvre, France), and

dimethylsulfoxide (DMSO) and formic acid (Prolabo, Paris, France) were all of analytical grade. Methanol-D4 and trifluoroacetic acid (TFA) were purchased from Sigma-Aldrich (St. Louis, MO, USA), and deuterium oxide (100.0 atom % D) and formic acid-D2 (99+ atom %, 95% solution in D_2O) from Acros Organics (Geel, Belgium). Water used throughout the experiments was generated by a Milli-Q water purification system (Milford, MA, USA).

Ammonium formate buffer was prepared by mixing ammonium formate and water to a concentration of 2 mM; the pH was adjusted to pH 3 ± 0.05 with formic acid.

Synthesis of metabolites M1, M2 and M6. Compounds M1, M2 and M6 were prepared as previously described.[13] All compounds were obtained as solids and the structures were confirmed by LC-MS/MS, ^{1}H, ^{13}C-spectra and 2D NMR experiments. Yields for the synthesis were not optimized. Methodological details are given in the data supplement.

NMR Spectroscopy. The NMR spectra of **EAPB203** and **EAPB202,** and that of the metabolites were obtained with a NM-40TH5 dual ^{1}H, ^{13}C probe in a JEOL EX400 operating at 400 MHz for proton and 100.53 MHz for carbon-13 at 298 K. ^{1}H and ^{13}C NMR chemical shifts are referenced to solvent peaks: δ_H 2.49 (residual DMSO-*d5*H) and δ_C 39.5 for DMSO-*d6*.

The assignment of all ^{1}H resonances was based on connectivity information transmitted via DQF ^{1}H-^{1}H COSY spectra. Assignment of the ^{13}C NMR resonances was performed by using HSQC (direct $^{1}J_{H\text{-}C}$ connectivities) and HMBC (long range $^{n}J_{H\text{-}C}$ couplings) experiments.

Two-dimensional (2D) homonuclear correlated experiments DQF-COSY and NOESY were all acquired using standard procedures with a spectral width of ca. 4000 Hz in both columns F1 and F2. The time domain matrix consisted of 256 points in t_1 and 1024-2048 points in t_2 with 64-128 acquisitions for 256 experiments in t_1. Data sets were zero-filled to 512 points in t_1 prior to Fourier transformation to obtain a frequency domain matrix of 512 x 1024-2048

real data points. Squared sine bell apodization functions were used. Heteronuclear correlated experiments were performed in ^{1}H-detected mode using the standard pulse programs HSQC and HMBC with a spectral width of ca. 20000 Hz in F1 and 4000 Hz in F2. The time domain matrix consisted of 256 points in t_1 and 2048 points in t_2 with 128 acquisitions for 256 experiments in t_1. Data sets were zero-filled to 512 points in t_1 prior to Fourier transformation to obtain a frequency domain matrix of 512 x 2048 real data points. The evolution delay was set to optimize 140 Hz couplings for HSQC and 8 Hz couplings for HMBC. Squared sine bell apodization functions were used.

QqQ MS/MS Fragmentation of EAPB0203 and EAPB0202 using the Syringe-Pump Method. MS/MS experiments were performed on an AB Sciex API 3000 triple quadrupole mass spectrometer (Courtaboeuf, France) with electrospray ionization (ESI) source. The ionisation mode was positive.

The stock solutions of **EAPB0203** and **EAPB0202** (1 g/L) were prepared in acetonitrile. They were extemporaneously diluted in acetonitrile-purified water-formic acid (50:49:1, v/v/v) to prepare working solutions at concentrations of 0.01 g/L. Working solutions were analyzed by direct continuous infusion (200 µL) at a flow rate of 10 µL/min using a syringe pump. Operating conditions were as follows: curtain gas, 10 psig; ion spray voltage, +6000V; entrance potential, 11 V; desolvatation temperature, 450 °C; declustering potential, 70 V; and focusing potential, 400 V. Nitrogen gas was used as the collision gas. Collision energy varied from 30 to 80 eV. The dwell time for each ion was set at 0.2 second.

We also performed H/D exchange studies that provide a convenient mean for elucidation of fragmentation mechanisms in MS/MS that is complementary to accurate mass

measurement. For which, samples were dissolved in methanol-D4 at concentration of 0.01 g/L. After a 2-hour incubation period at 20 °C in the dark, they were infused into the source.

High resolution MS and MS^2 Analyses of Directly Infused EAPB0203 and EAPB0202. For the determination of exact masses, a Q-Tof I mass spectrometer (Waters, Milford, CA) fitted with an ESI ion source was used. The mass spectrometer was calibrated in the positive ion mode using 1% phosphoric acid in H_2O/CH_3CN solution (50:50, v/v). Data were acquired by the Tof analyzer at 1 acquisition/s from *m/z* 50 to *m/z* 3000 with a resolution of 7500. Depending on the sample, three to eight acquisitions were summed to produce the final spectrum. Samples were dissolved as previously described and infused into the ESI source at a flow rate of 5 µL/min. The following MS conditions were used: voltages were set at +3.0 kV for the capillary and adjusted for the sampling cone from 10 to 60 V according to the sample. The source was heated at 100 °C. Nitrogen constituted both nebulizing and desolvatation gas. The latter was heated at 120 °C. In MS/MS experiments, the sampling cone was set at 50 V. The second quadrupole analyzer was set in the rf mode using argon as collision gas and the collision energy varied from 10 to 30 eV depending on the samples to give optimal fragmentation. MassLynx v. 4.1 (Waters) software was used for data acquisition and processing.

LC-MS/MS (QqQ) Method for the Separation and Identification of Metabolites of EAPB0203. The LC system (Agilent 1200 LC, Agilent Technologies, Les Ulis, France) was connected to the API 3000 tandem triple quadrupole mass spectrometer. MS conditions were similar to those described above. LC separations were performed using a method similar to that previously published.[7] The column used was a C8 Zorbax eclipse XDB (5 µm, 4.6 mm × 150 mm) preceded by a guard column of the same nature (3.9 mm × 20 mm)

(Agilent Technologies), both maintained at 40 °C. Chromatography was carried out via a gradient system; the flow rate was set at 800 µL/min. The eluent was post-column split and approximately 0.5 mL/min was directed to the LC-MS interface. Mobile phase A was acetonitrile and mobile phase B contained 2 mmol/L ammonium formate buffer (pH 3.0 ± 0.05). The gradient elution was employed according to the following linear programme: time zero, 30% solvent A; 9 min, 100% solvent A; 10 min, 100% solvent A; 11 min, 30% solvent A; and 14 min, 30% solvent A. The autosampler was maintained at 4 °C.

Incubation of EAPB0203 and EAPB0202 with Rat and Dog liver microsomes. EAPB0203 and **EAPB0202** (20 µM) were incubated with 1 g/L of pooled rat and dog liver microsomal proteins in 0.1 M phosphate buffer solution (pH 6.3) as previously described.[8] Reactions were initiated by addition of NADH (10 mM). The incubations were carried out at 37 °C in a shaking incubator. The total incubation mixture volume was 250 µL. After incubation for 4 h, 0.25 mL of purified water and 0.5 mL of water containing 10 mL/L TFA were added. After centrifugation (4 °C) for 10 min at 4000*g*, the sample pretreatment procedure was the same as that published previously.[7] Briefly, the supernatants were transferred onto preconditioned Oasis HLB cartridges (30 mg). The cartridges were then washed with 1 mL of water and the analytes were eluted with 2x1 mL of dichloromethane. The eluates were evaporated to dryness under nitrogen at 40 °C. The residues were reconstituted with 100 µL of a mixture containing acetonitrile-water-formic acid (50:49:1, v/v/v) then 10 µL were injected into the LC-MS/MS system. All determinations were performed in triplicate on three different days.

Incubation of EAPB0203 and EAPB0202 with *Cunnighamella Elegans.* Stock culture of *C. elegans* ATCC 36112 (LGC Standards, Molsheim, France) was maintained on Sabouraud

dextrose agar plates at 4 °C. Spores and/or mycelia were used to inoculate 125-mL Erlemmeyer flasks containing 30 mL of Sabouraud dextrose medium. After 48-h incubation at 25 °C on a rotary shaker (150 rpm), the mycelia were removed and transferred to 125-mL Erlemmeyer flasks containing 30 mL of Sabouraud. 0.5 milligram of **EAPB0203** or **EAPB0202** dissolved in 100 µL DMSO (i.e., 1.65 and 1.73 µmol, respectively) was added to each flask (4 flasks per compound). Control included an incubation of the fungus without the drugs (2 flasks). All of the flasks were incubated at 25 °C for 168 h. Thereafter mycelium was separated from the culture broth by filtration. Under these conditions, **EAPB0203** and **EAPB0202** were found to be stable. After lyophilisation of the media, the pellets were extracted with dichloromethane (2 mL) then with 1 mL of a mixture dichloromethane/methanol (50:50, v/v). The organic phases were evaporated to dryness under a stream of nitrogen (40 °C). Each residue was dissolved in 0.3 mL DMSO, and then 2.7 mL of water containing 5 mL/L TFA were added. Purification was accomplished by means of solid-phase extraction. Thus, each solution was loaded onto Oasis HLB 60 mg cartridges previously conditioned with 2 mL of methanol and equilibrated with 2 mL of water. The cartridges were washed with 2x1.5 mL of purified water. The analytes were eluted with 3x2 mL of dichloromethane. Eluates were combined then evaporated to dryness under nitrogen at 40 °C. The residues were finally redissolved in 5 mL of a mixture containing acetonitrile-water-formic acid (50:49:1, v/v/v) then 5 µL were injected into the LC-MS/MS system. These determinations were replicated on two different days.

■ RESULTS AND DISCUSSION

Nuclear magnetic resonance (NMR) spectroscopy. Structure and NMR assignments of **EAPB0203** and **EAPB0202** are presented in supplemental data Figure 3A,B. The ^{1}H NMR spectrum (400 MHz, DMSO-*d6*) of **EAPB0202** showed eleven signals ascribable to ten aromatic protons, four aliphatic ones and two exchangeable protons. Interpretation of ^{1}H-^{1}H DQF-COSY spectrum suggested that these eleven signals could be assigned to the three isolated spin systems (H6-H7-H8-H9, H1'-H2', and H4'-H5'-H6'-H7'-H8'), the isolated proton (H2) and to the two amine protons. The ^{13}C NMR (100 MHz, DMSO-*d6*) spectrum showed 6 quaternary carbons, eight sp^2 carbons, and two sp^3 carbons. HMQC and HMBC connectivities allowed the unambiguous assignments of all proton and carbon resonances to the structure of **EAPB0202**. In the ^{1}H NMR spectrum, the multiplicity of the two methylene groups, H1' and H2', two triplets instead of two AB systems, clearly indicated the presence of two pairs of equivalent protons and consequently a free rotation around the bonds C1-C1', C1'-C2' and C2'-C3'. But, analysis of through-space interactions observed in NOESY experiment (supplemental Figure 3A) showed two nOe cross-peaks H2/H2’ and H1’/H9 (orange arrays in 3D **EAPB202** structure). This seems to indicate that a preferential conformation occurs, in DMSO, with the three bonds C1-C1', C1'-C2' and C2'-C3' in the plane of the tricyclic aromatic ring system. As expected, **EAPB0203** showed remarkable NMR spectral similarities to **EAPB0202**, the most significant differences being the presence of an additional signal corresponding to the *N*-methyl group. COSY, HSQC and HMBC NMR spectra are presented in supplemental data Figure 4A,B.

MS/MS fragmentations of EAPB0203 and EAPB0202. Results of the ESI-MS/MS analyses carried out on the QqTof mass spectrometer are tabulated in supplemental Table 1. High

resolution experiments were performed for both **EAPB0203** and **EAPB0202** compounds on the protonated molecular ion and some of the observed fragment ions. The elemental compositions of the selected precursor ions and of fragment ions were deduced from the measured exact masses. The mass errors between the theoretical calculated and measured masses ranged from 2 to 11 ppm, which indicated relatively good mass accuracies. QqTof-MS/MS spectra of the $[M_H+H]^+$ precursor ions at *m/z* 303 (**EAPB0203**) and *m/z* 289 (**EAPB0202**) are shown in supplemental data Figures 5 and 6 that accompany this paper, respectively. Very surprisingly, MS/MS spectra showed that both protonated molecules possessing an even number of electrons were unexpectedly losing radicals such as $H^{\bullet}$ (loss of 1 Da), $CH_3^{\bullet}$ (loss of 15 Da) or even $C_7H_7^{\bullet}$ (loss of 91 Da) giving stable radical cations. Such assignments were unambiguously confirmed by exact mass measurements of the observed fragment ions as shown in supplemental Table 1. The loss of $H^{\bullet}$ was very weak and was clearly detected under QqTof MS/MS experiments. Besides, the 91 mass loss was tricky to be identified as the tropyl radical ($C_7H_7^{\bullet}$) being isobaric with the neutral molecule C_6H_5N (91 Da) that can be formally lost from the fused benzene ring side. Following elucidation of the fragmentation mechanisms using ESI-QqTof-MS^2 experiments supported by exact mass measurements, we can propose, for **EAPB0203** and **EAPB0202,** the fragmentation schemes illustrated in Figure 1. Stabilization of distonic radical cations is allowed by delocalisation of the radical as shown by the variety of isomeric forms that can be suggested, which explained the propensity of such heterocyclic compounds to spontaneously fragment upon low energy collision-induced dissociations to form radicals.

H/D exchange experiments on EAPB0203 and EAPB0202. H/D exchange experiments were conducted on the QqQ. When **EAPB0203** was dissolved in methanol-D4, it generated

an $[M_D+D]^+$ ion at *m/z* 305. The 2 Da increase is in agreement with the presence of one exchangeable hydrogen atom in its structure and the supplemental 1 Da being contributed by the ionizing agent D^+. The MS/MS spectrum of the *m/z* 305 ion afforded predominant fragment ions at *m/z* 214, *m/z* 199/198, *m/z* 172/171 and *m/z* 129/128 thus confirming the fragmentation pathway deduced from the high resolution MS experiments. Concerning the metabolite **EAPB0202,** the $[M_D+D]^+$ ion was at *m/z* 292; the 3Da increase is in agreement with the exchange of two hydrogen atoms by deuterium and the presence of one deuterium affording the ionized species. The MS/MS spectrum of the *m/z* 292 ion gave the following predominant fragment ions: *m/z* 201/200 and *m/z* 174/173/172 indicative of the presence of two to three exchangeable hydrogen atoms in these fragments; other predominant fragment ions were *m/z* 129/128 and *m/z* 118/117. Results of H/D exchange experiments are reported in Table 1. These results were in agreement with the fragmentation schemes shown in Figure 1.

LC-MS/MS Experiments. After incubation of **EAPB0203** with dog and rat liver microsomes, 71.3±2.9 and 57.0±1.7% (n=9) of the drug were metabolized, respectively. The LC-MS analysis of the extracts carried out on the ESI-QqQ mass spectrometer allowed identification of four major metabolites (**EAPB0202,** M7, M2 and M1, supplemental Figure 7A) in dog and six metabolites (**EAPB0202,** M7, M6, M3, M2 and M1, supplemental Figure 7B) in rat. After incubation of **EAPB0202**, two metabolite peaks were generated both in dog (M5 and M1, 75±3.0% of **EAPB0202** metabolized, supplemental Figure 7C) and in rat (M3 and M1, 55±2.5% of **EAPB0202** metabolized, supplemental Figure 7D). The retention times of **EAPB0203**, **EAPB0202**, M7, M6, M5, M3, M2 and M1 were 6.56, 5.62, 4.8, 4.34, 4.28, 4.11, 4.08, and 3.57 min, respectively (supplemental Figure 7). They were detected as their

$[M_H+H]^+$ ions at *m/z* 303 (**EAPB0203**), 289 (**EAPB0202**), 319 (M7, M6 and M2; 16 Da higher than the protonated molecular ion of **EAPB0203**) and 305 (M5, M3, M1; 16 Da higher than the protonated molecular ion of **EAPB0202**). Thus, M7, M6 and M2 are oxygenated derivatives of **EAPB0203**, and M5, M3 and M1 that of **EAPB0202**. LC-MS/MS analysis of the extracts from cultures of *C. elegans* grown with **EAPB0203** and **EAPB0202** allowed identification of two peaks from **EAPB0203** which eluted at 4.08 min (M2, *m/*z 319) and 3.57 min (M1, *m/*z 305), and one peak from **EAPB0202** (M1, *m/*z 305) which eluted at 3.57 min (supplemental Figure 8). On-line H/D exchange LC-MS/MS was also performed using D_2O and formic acid-D2 in the mobile phase as well as for the reconstitution of the extracts to aid in identification of the metabolite structures and to discriminate between hydroxylation and *N*-oxidation (Table 1). The structures of metabolites were elucidated based on the combination of different techniques: (i) their fragmentation pathways in LC-MS/MS; (ii) the comparison of their changes in their molecular masses and fragment ions with those of the parent drugs; and (iii) the results of H/D exchange experiments. Although the retention time was slightly shifted with deuterated solvents, metabolites were traced by mass measurements. For M6, M2 and M1 comparisons with authentic standards in LC-MS/MS were performed to confirm the structures.

Identification of metabolites M2 and M1. M2 was produced by dog and rat hepatic microsomal preparations containing **EAPB0203** (supplemental Figure 7A,B) and M1 was formed in microsomes from rat and dog containing **EAPB0203** and **EAPB0202** (supplemental Figure 7). When H_2O was used as the aqueous component in the mobile phase, M2 and M1 gave $[M_H+H]^+$ molecular ions at *m/z* 319 and 305, respectively. When molecular ions of M2 and M1 were fragmented upon collision induced dissociations (30-80 eV), they not only

showed the same fragmentation ions as **EAPB0203** and **EAPB0202**, but also displayed ion intensities similar to those of **EAPB0203** and **EAPB0202** in the MS/MS spectra, respectively (supplemental Table 2). Ions at *m/z* 212 and 198 were produced through loss of the radical $C_7H_7O^{\bullet}$ from the molecular ions, respectively. These results suggested that the mass increment of 16 Da occurred on the phenethyl moiety of the parent compounds. The retention times and fragmentation patterns of M2 and M1 found in the extracts from cultures of *C. elegans* were well in agreement with those of M2 and M1 found after incubation of **EAPB0203** and **EAPB0202** with hepatic microsomes. Noninoculated controls without the drugs had no peaks corresponding to any of the two metabolites. The on-line H/D exchange LC-MS/MS experiments using D_2O and formic acid-D2 afforded $[M_D+D]^+$ ions at *m/z* 322 for M2 (predominant fragment ions at *m/z* 214, 199 and 172) and *m/z* 309 for M1 (predominant fragment ions at *m/z* 201, 173/172 and 129/128) (Table 1). This revealed that M2 had three exchangeable hydrogen atoms and M1 four exchangeable hydrogen atoms in their structures. Thus, M2 and M1 could be formed by aromatic hydroxylation of the phenyl ring D (supplemental Figure 1). Based on LC-MS/MS spectra and coelution with available standards, M2 and M1 were hydroxylated at the C-6' position of the ring D. M1 is the demethylated compound of M2.

Identification of metabolites M6 and M3. When H_2O was used in the mobile phase, M6 (found in the rat microsomes incubated with **EAPB0203**, supplemental Figure 7B) gave rise to a pseudo-molecular ion at *m/z* 319. At collision energy of 30 eV, one product ion was obtained at *m/z* 228 $[M_H+H-C_7H_7^{\bullet}]^{+\bullet}$. At 50 eV, the following product ions were observed: *m/z* 228 and the further loss of $H^{\bullet}$ (*m/z* 227), *m/z* 213 and 201 by loss of $CH3^{\bullet}$ and HCN from *m/z* 228, respectively. At 80 eV, the most abundant fragment ions were detected at *m/z* 213,

186/185, 145/144 and 133 (supplemental Table 2). M3 (found in the rat microsomes incubated with **EAPB0203** and **EAPB0202**, supplemental figure 7B,D) gave protonated molecule at *m/z* 305. For the MS/MS experiment, the molecular ion was fragmented at collision energy of 30 eV, which formed daughter ion fragment at *m/z* 214 corresponding to the loss of the tropyl radical. At collision energy of 50 eV, other fragment ions were generated from *m/z* 214: *m/z* 213, 197 and 187 by the loss of $H^{\bullet}$, NH_3 and HCN, respectively; the ion at m/z 213 also loosing HCN to give m/z 186. At higher collision energy (such as 80 eV), product ions were similar to those already observed for M6 but with slightly different relative abundances (supplemental Table 2). For both M6 and M3, all detected fragment ions were exhibiting a mass increment of 16 Da compared to those formed from **EAPB0203** and **EAPB0202**, respectively and were detected with similar percent relative abundances. Thus, the incorporation of an oxygen atom had occurred on the phenyl ring A of the quinoxaline ring (supplemental Figure 1). M3 is the demethylated compound of M6. The MS/MS spectrum of M6 in D_2O gave the $[M_D+D]^+$ ion at *m/z* 322 indicating the presence of three exchangeable hydrogen atoms in the structure. At 30-80 eV, the main product ions were: *m/z* 231 $[M_D+D-C_7H_7^{\bullet}]^{+\bullet}$, *m/z* 216 (loss of $CH3^{\bullet}$ from *m/z* 231) and *m/z* 188 (loss of DCN from *m/z* 216) (Table 1). In D_2O, M3 was detected at *m/z* 309 suggesting four exchangeable hydrogen atoms in its structure; the most abundant product ions were *m/z* 218 ($[M_D+D-C_7H_7^{\bullet}]^{\bullet+}$), 217 by loss of $H^{\bullet}$, 190 by loss of DCN, 189 (losses of $H^{\bullet}$ and DCN) and 146/145 (Table 1). Based on these results, M6 and M3 can be rationalized as hydroxylated metabolites. M6 was identified by LC-MS/MS co-analysis with synthetic standard. NMR experiments, ^{1}H NMR and NOE DIFF, confirmed the proposed structure for M6, with the site of hydroxylation clearly located on position C8 (supplemental Figure 9).

Identification of metabolites M7 and M5. M7 (found in the dog microsomes incubated with **EAPB0203**, supplemental Figure 7A) gave a pseudo-molecular ion $[M_H+H]^+$ at *m/z* 319 which fragmented to *m/z* 228 $[M_H+H-C_7H_7^{\bullet}]^{+\bullet}$, *m/z* 227 by further loss of $H^{\bullet}$, and *m/z* 213 by loss of $CH3^{\bullet}$ using a collision energy of 50 eV. These product ions have a mass difference of 16 Da relative to the fragment ions of *m/z* 212, 211 and 197 formed from **EAPB0203** (supplemental Table 2). Thus, the oxygen atom should be positioned on the imidazoquinoxaline ring. This collision energy gave informative structural data since other fragments detected at *m/z* 199 and 185 were generated from *m/z* 227 and 213 by the loss of CO, respectively. In contrast to metabolite M6 where the incorporation of the oxygen atom had occurred on the phenyl ring A of the quinoxaline ring leading to the loss of 27 Da (HCN) from the same fragment ions, such neutral loss of 28 Da (CO) clearly indicated that the hydroxyl group was precisely located onto the imidazole ring as seen in Figure 2. At 80 eV, predominant product ions were: *m/z* 227, 213/212, 199/198, 185/184, 171/170, 144/143, and 131/130/129/128 (supplemental Table 2). The demethylated product of M7, M5, found after incubation of **EAPB0202** with the dog hepatic microsomes (supplemental Figure 7C) gave protonated molecule at *m/z* 305. MS/MS spectra (collision energy, 30 eV) revealed daughter ion fragment at *m/z* 214 $[M_H+H-C_7H_7^{\bullet}]^{+\bullet}$. At 50 eV, the loss of $H^{\bullet}$ and NH_3 from the ion at *m/z* 214 leads to fragment ions at *m/z* 213 and 197, respectively. As previously reported for M7, at 80 eV, the abundant fragment with *m/z* 185 resulted from the loss of CO from *m/z* 213. At this high collision energy, most of the obtained fragment ions were similar to those observed for M7. Results are presented in supplemental Table 2. The proposed fragmentation pathway is depicted in Figure 2. These data indicated that, for both M7 and M5, the oxygen atom was positioned at the C-2 position on the imidazole C ring. Compared

to **EAPB0203** that yielded an abundant signal at *m/z* 212 by loss of the tropyl radical (intensity, 98%) while that at *m/z* 211 was not very pronounced (<5%), the presence of the hydroxyl group on the imidazole ring decreased the stability of the radical cation at m/z 228 (20%) and high abundant fragment ion at m/z 227 (100%) was observed (supplemental Table 2). The MS/MS spectrum of M7 in D_2O afforded the *m/z* 322 ion (corresponding to the *m/z* 319 in H_2O) indicating that there were three exchangeable hydrogen atoms on this structure. Predominant fragment ions were: *m/z* 231/230/229, 216/215/214, 201/200 and 188/187/186 (Table 1). Concerning M5, on-line H/D exchange LC-MS/MS experiment produced $[M_D+D]^+$ ion at *m/z* 309, suggesting four exchangeable hydrogen atoms. Predominant fragment ions were: *m/z* 218/217/216 and 188/187/186 (Table 1). These data confirmed that M7 and M5 were obtained by hydroxylation and were in agreement with the fragmentation schemes shown in Figure 2. The MS/MS spectra combined with accurate mass measurements provided rapid and reliable information to identify the C-2 location of the hydroxyl group on the C ring of the parent molecules.

■ CONCLUSION

In the present study, LC-MS/MS with QqTof mass analyzer configuration was used to identify all fragment ions of **EAPB0203** and **EAPB0202**. Most measured mass errors were less than 10 ppm using external mass calibration, indicating high mass accuracy. The combination of different analytical techniques was used to elucidate the structures of oxygenated metabolites of the two parent compounds. All of them were hydroxylated compounds. This was confirmed by on-line H/D exchange LC-MS/MS experiments which clearly facilitate the differentiation of hydroxylated metabolites from N-oxydes. Structures of M1, M2 and M6

have been assigned based on LC-MS/MS techniques together with comparison with synthetic standards. The chemical structures of these standards were confirmed by LC-MS/MS and NMR analyses. Structures of M5 and M7 were confirmed by LC-MS/MS and accurate mass measurement. Using cryopreserved rat, dog and human hepatocytes, we have found that hydroxylated metabolites were partially further conjugated with glucuronic acid (data not shown).

■ ACKNOWLEDGEMENTS

The authors would like to thank Bénédicte Marion and Jacques Bompart for their assistance.

This work was partially supported by the Gefluc Languedoc-Roussillon, Montpellier, France.

■ ASSOCIATED CONTENT

Supporting Information.

This material is available free of charge via the Internet at http://pubs.acs.org.

■ AUTHOR INFORMATION

Corresponding Author

*E-mail: FBressolle@aol.com. Tel: (33) 4 11 75 95 76. Fax: (33) 4 11 75 97 37

*carine.masquefa@univ-montp1.fr (tel) (33) 4 11 75 95 36; (fax) 33 4 11 75 95 53

REFERENCES

(1) Steinmann, A.; Funk, J.O.; Schuler, G.; Von den Driech, P. *J. Am. Acad. Dermatol*. **2000**, *43*, 555-556.

(2) van Egmond, S.; Hoedemaker, C.; Sinclair, R. *Int. J. Dermatol.* **2007**, *46*, 318–319.

(3) Moarbess, G.; Deleuze-Masquéfa, C.; Bonnard, V.; Paniagua, S.; Vidal, J.R.; Bressolle, F.; Pinguet, F.; Bonnet, P.A. *Bioorg. Med. Chem.* **2008**, *16*, 6601-6610.

(4) Moarbess, G.; El-Hajj, H.; Kfoury, Y.; El-Sabban, M.E.; Lepelletier, Y.; Hermine, O.; Deleuze-Masquéfa, C.; Bonnet, P.A.; Bazarbachi, A. *Blood* **2008,** *111*, 3770-3777.

(5) Deleuze-Masquéfa, C.; Moarbess, G.; Khier, S.; David, N.; Gayraud-Paniagua, S.; Bressolle, F.; Pinguet, F.; Bonnet, P;A. *Eur. J. Med. Chem.* **2009,** *44*,3406–3411.

(6) Khier, S.; Moarbess, G.; Deleuze-Masquéfa, C.; Margout, D.; Solassol, I.; Pinguet, F.; Bonnet, P.A.; Bressolle, F. *J. Sep. Sci.* **2009**, *32:1363-1373.*

(7) Khier, S.; Deleuze-Masquéfa, C.; Moarbess, G.; Gattacceca, F.; Margout, D.; Solassol, I.; Cooper, J.F.; Pinguet, F.; Bonnet, P.A.; Bressolle, F.M. *Eur. J. Pharm. Sci.* **2010**, *39*:23-29.

(8) Khier, S.; Gattacceca, F.; El Messaoudi, S.; Lafaille, F.; Deleuze-Masquéfa, C.; Bompart, J.; Cooper, J.F.; Solassol, I.; Pinguet, F.; Bonnet, P.A.; Bressolle, F.M.M. *Drug Metab. Dispos.* **2010**, *38*, 1836-1847.

(9) Ohashi, N.; Furuuchi, S.; Yoshikawa, M. *J. Pharm. Biomed. Anal*. **1998**, *18*, 325-334.

(10) Liu, D.Q.; Hop, C.E.; Beconi, M.G.; Mao, A.; Chiu, S.H. *Rapid Commun. Mass Spectrom*. **2001**, *15*, 1832-1839. *Erratum in*: *Rapid Commun. Mass Spectrom*. **2003**, *17*, 264.

(11) Asha, S.; Vidyavathi, M. *Biotechnol. Adv.*, **2009**, *27*, 16-29

(12) Masquéfa, C.; Moarbess, G.; Bonnet, P.A.; Pinguet, F.; Bazarbachi, A.; Bressolle, F. Patent Corporation Treaty; European patent, 2008/063290.

(13) Deleuze-Masquefa. C.; Gerebtzoff, G.; Subra, G.; Fabreguettes, J.R.; Ovens, A.; Carraz, M.; Strub, M.P.; Bompart, J.; George, P.; Bonnet, P.A. *Bioorg. Med. Chem.* **2004**,12,1129-1139.

Legends of Figures

Figure 1. Proposed fragmentation pathways of **EAPB0203** and **EAPB0202.**

Figure 2. Proposed fragmentation pathways of M7 and M5.

Table 1 LC-MS/MS behavior of **EAPB0203**, **EAPB0202** and their metabolites after H/D exchanges in triple quadrupole in the positive ionization mode.

	Collision energy (eV)	Precursor Ion	Ion fragments[a,b]
EAPB0203 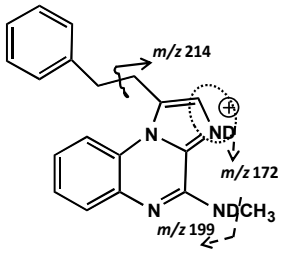 rt=6.82 min	30	305 (100%)	**214** (60%).
	50	None	**214** (80%)/213 (20%), **199** (100%)/198 (37%), 187 (10%).
	80	None	213 (15%), **199** (75%)/198 (44%), **172** (100%)/**171** (83%)/170 (20%), 154 (40%), 144/143 (40%), **129/128 (50%)**, 118/117 (25%), 102 (15%).
EAPB0202 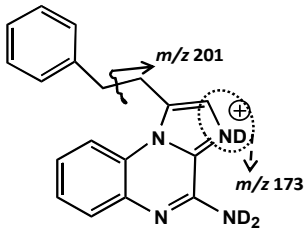 rt=5.71 min	30	292 (100%)	**201** (50%).
	50	None	**201** (100%)/**200** (65%)/199 (10%), 181 (10%), 174 (10%)/173 (10%).
	80	None	**200** (63%)/199 (25%), **173** (75%)/**172** (100%)/171 (24%), 154 (30%), 145 (40%)/144 (27%), **129/128** (65%), **118/117** (55%), 103/102 (50%).
M1 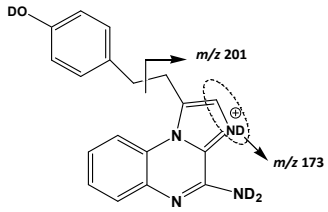 rt = 3.74 min	30	309 (100%)	**201** (74%).
	50	None	**201** (100%)/200 (30%), 181 (10%), 174 (10%)/173 (10%).
	80	None	200 (43%)/199 (10%), **173** (65%)/**172** (100%)/171 (20%), **129/128** (60%), 118/117 (45%), 102/103 (30%).
M2 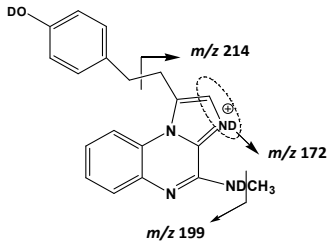 rt = 4.28 min	30	322 (87%)	**214** (100%).
	50	None	**214** (100%)/213 (20%), **199** (63%)/198 (15%), 187 (5%).
	80	None	213 (5%), **199 (60%)**/198 (5%), **172** (100%)/171 (42%), 129/128 (30%), 118/117 (15%).
M3 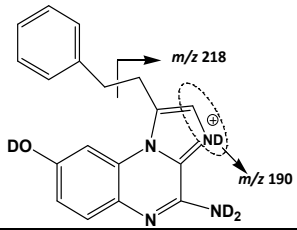	30	309 (100%)	**218** (60%).
	50	None	**218** (100%)/**217** (70%), 198 (10%), 190 (10%).
	80	None	**217** (50%), **190/189** (100%), 161/160 (40%), **146/145** (53%), 135/134 (30%)

rt = 4.34 min			
M5 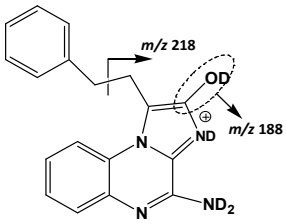 rt = 4.36 min	30 50 80	309 (88%) None None	**218 (100%)** **218** (57%)/**217** (100%), 198 (22%), **188** (50%) **217** (100%)/216 (40%), 188/187/186 (30%), 133/132/131/130 (30%).
M6 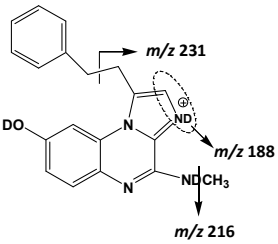 rt = 4.48 min	30 50 80	322 (100%) None None	**231** (50%)**.** **231** (100%)/230 (10%), **216** (90%)/215 (18%)**,** 204 (10%) / 203 (10%). **216** (60%), **188** (100%)/187 (40%), 161/160 (28%), 146/145 (45%), 134/133 (35%).
M7 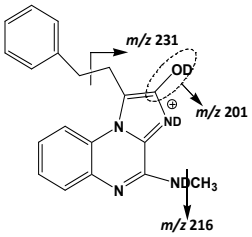 rt = 5.05 min	30 50 80	322 (75%) None None	**231** (100%) 231 (20%)/**230** (100%), 216/215 (20%), 201/200 (40%), **188/187/186** (50%). **230**/229 (100%), **216/215/214** (50%), 201/200 (40%), 188/187/186 (40%), 172 (30%), 160/159/158 (25%), 145/144 (45%), 133/132/131/130 (30%).

Similar fragmentation patterns were obtained in rat and dog.

[a]Boldface indicates the most prominent product ion(s); [b]Values in parentheses are relative peak intensities. rt, retention time. Retention times were slightly shifted with deuterated solvents

FOR TOC ONLY

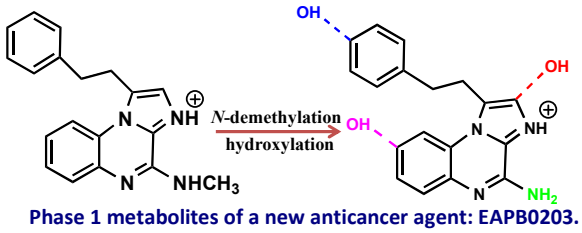

Phase 1 metabolites of a new anticancer agent: EAPB0203. NMR and LC-MS/MS analyses

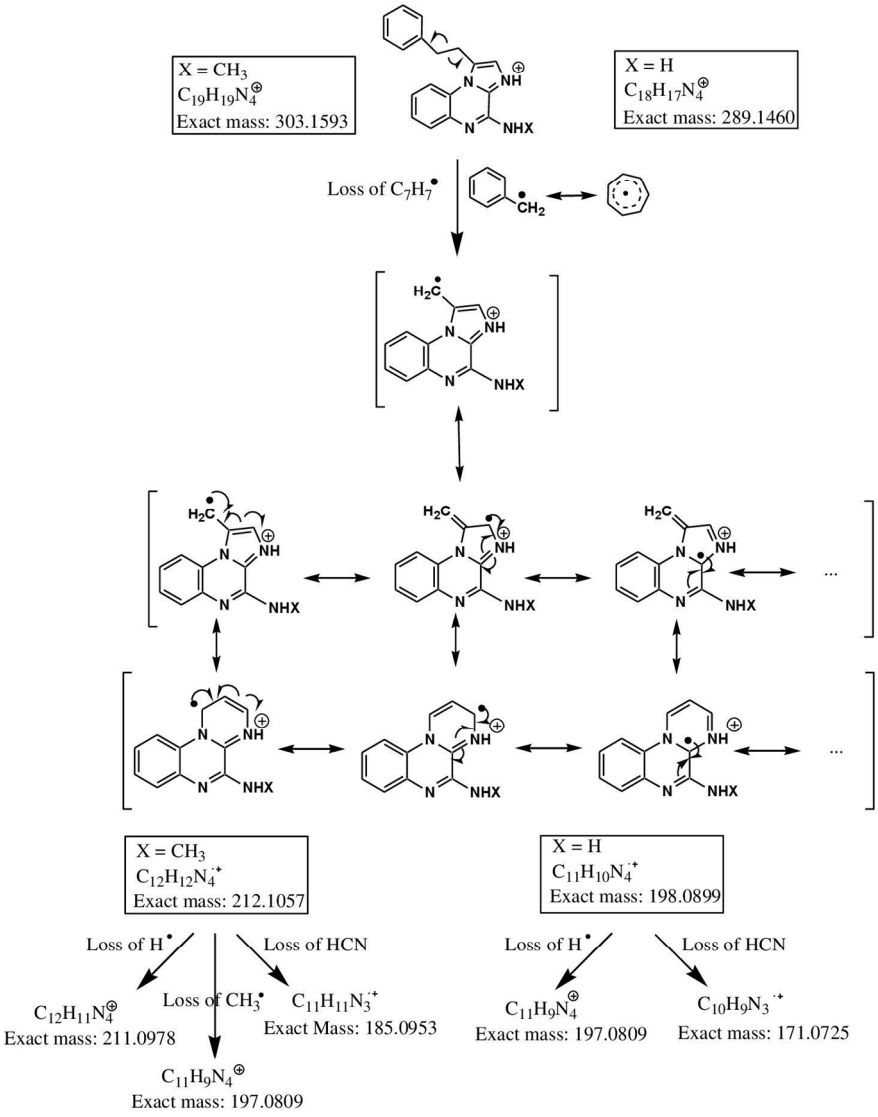

Proposed fragmentation pathways of EAPB0203 and EAPB0202.
396x529mm (96 x 96 DPI)

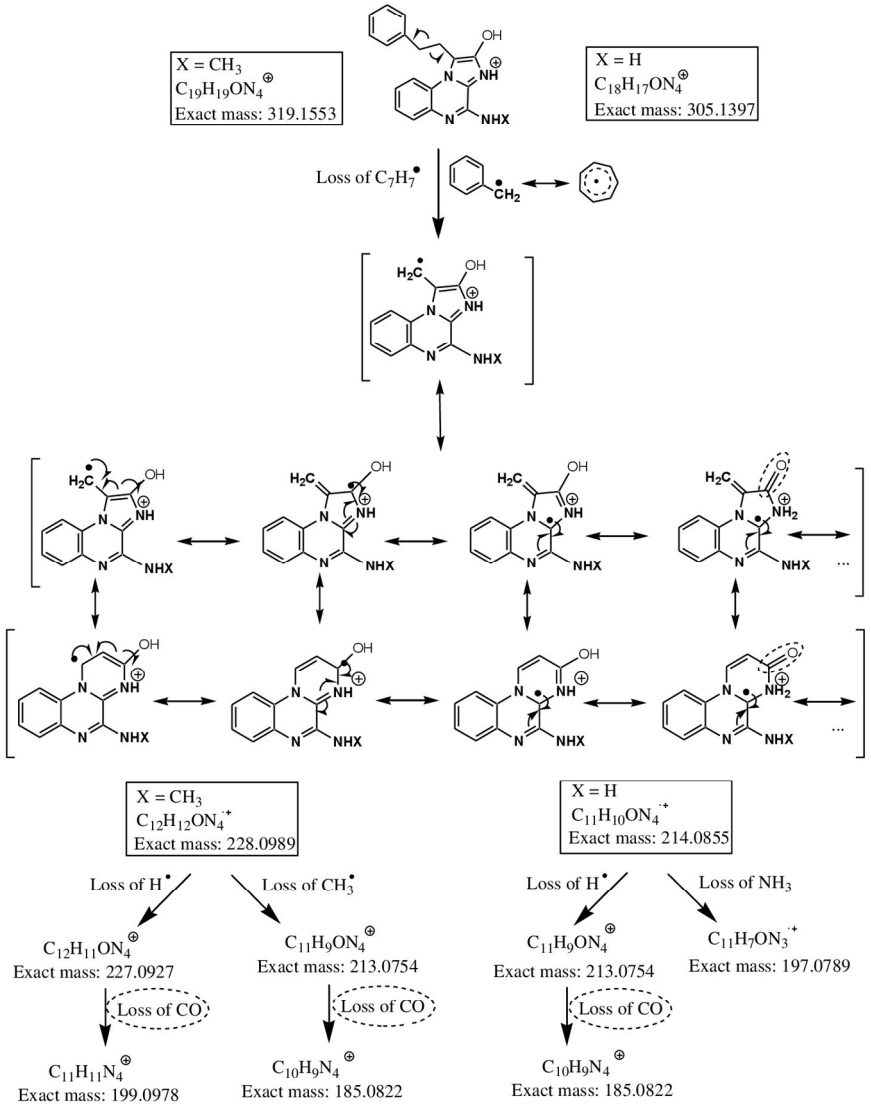

Proposed fragmentation pathways of M7 and M5.
396x529mm (96 x 96 DPI)